DOE/NV/25946--224

FLASH X-RAY DIFFRACTION SYSTEM FOR FAST, SINGLE-PULSE TEMPERATURE AND PHASE TRANSITION MEASUREMENTS

Dane V. Morgan,[ξ] Don R. Macy, Michael J. Madlener, and Jiaming G. Morgan
National Security Technologies, LLC, 182 East Gate Drive,
Los Alamos, NM 87544 USA

Abstract

A new, fast, single-pulse diagnostic for determining phase transitions and measuring the bulk temperature of polycrystalline metal objects has been developed. The diagnostic consists of a 37-stage Marx bank with a cable-coupled X-ray diode that produces a 35-ns pulse of mostly 0.71-Å monochromatic X rays and a P-43 fluor coupled to a cooled, charge-coupled device camera by a coherent fiber-optic bundle for detection of scattered X rays. The X-ray beam is collimated to a 1° divergence in the scattering plane with the combination of a 1.5-mm tungsten pinhole and a 1.5-mm-diameter molybdenum anode. X rays are produced by a high-energy electron beam transiting inward from the cathode to the anode in a needle-and-washer configuration. The anode's characteristic K-α X-ray emission lines are utilized for this diffraction system. The X-ray anode is heavily shielded in all directions other than the collimated beam. The X-ray diode has a sealed reentrant system, allowing X rays to be produced inside a vacuum containment vessel, close to the sample under study.

I. INTRODUCTION

X-ray diffraction (XRD) is a useful diagnostic for unequivocal determination of solid-solid and solid-liquid phase transitions. However, for a dynamic high-explosive or gun-driven experiment, the effective shock-loaded observation time is on the order of 100 ns. Therefore, standard commercial XRD machines are ineffective because of insufficient X-ray flux. XRD may be observed on this timescale by laser-driven plasma X-ray sources; however, the source size necessary to produce sufficient flux at X-ray energies above 15 keV may be cost-prohibitive. In contrast, our single-pulse electron beam X-ray source will produce characteristic 17.4- and 22.1-keV line emission of sufficient intensity to observe XRD on this short timescale using a low-cost, portable system.

Single-pulse XRD also enables direct, fast, bulk-temperature measurements of the sample under study. According to Debye and Waller [1], diffracted line intensity decreases as sample temperature increases, with no corresponding change in line width. As the sample temperature increases, the atoms' random displacement from their equilibrium lattice position increases. This displacement of the scattering atoms causes a phase shift that reduces the Bragg-reflected wave intensity. In principle, the Debye-Waller factor can be used to perform temperature measurements on our single-pulse XRD system's timescale.

In this paper we describe our newly designed, single-pulse XRD system. We have incorporated important system design features that enable single-pulse XRD, including a unique anode-pinhole collimator, high-energy X-ray diode shielding, and a low-noise imaging detector system. The X-ray source has been shown to provide sufficient characteristic line emission to observe polycrystalline metal Bragg diffraction patterns with a 35-ns X-ray pulse. The system has been tested in the laboratory with samples of indium and tin heated on a hot plate. Upon melt, diffraction lines have been observed to disappear; however, background from Compton scattering and sample fluorescence remained in the image. We have successfully tested the fast temperature measurement diagnostic with a single-pulse, 0.71-Å XRD image from the aluminum (400) line on a hot plate, at temperatures of up to 300°C. These experimental results are compared with the harmonic approximation for aluminum [2].

II. EXPERIMENTAL APPARATUS

A schematic diagram of the experimental apparatus appears in Figure 1. National Security Technologies, LLC, designed and built a 37-stage, 8.1-nF Marx bank used for these experiments. The stages were charged to 30 kV, then triggered to discharge in series into a remote

[ξ]email: morgandv@nv.doe.gov

needle-and-washer X-ray diode through a 40-Ω, DS-2158 coaxial transmission line. Because the 17.4-keV molybdenum and 22.1-keV silver emission line energies are much lower than the potential developed across the A-K gap, the load impedance was reduced to increase the emission current. We employed a 5-mm-diameter cathode and a 1.5-mm-diameter anode with a conical tip. This cathode diameter is smaller than cathodes typically used in radiographic X-ray diodes. In this configuration, we estimated the peak voltage across the diode at slightly less than 400 kV. The anode survived approximately five shots before refurbishment was required.

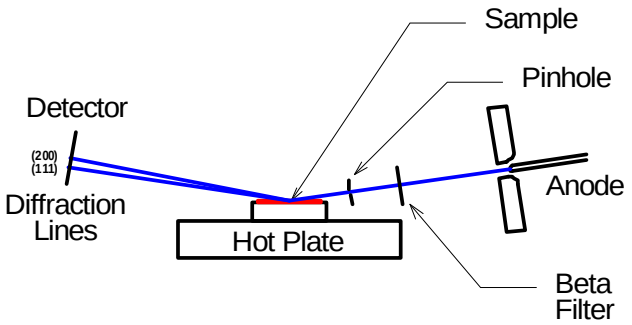

Figure 1. In the experimental setup, the lowest-order diffraction lines for aluminum are shown at the scattering angles for a 0.71-Å molybdenum K-α X-ray emission.

The X-ray diode was specially designed for diffraction studies, with a short vacuum transmission line section and a heavily shielded A-K gap. Sufficient shielding effectively eliminated direct X rays with energies of up to 400 keV outside the diode in all directions, except through the pinhole collimator. We successfully obtained single-pulse XRD images using molybdenum and silver anodes. The characteristic K-α wavelengths and K-β filters used with these anodes appear in Table 1. To produce a collimated X-ray beam, a rectangular tungsten pinhole was placed ~70 mm from the anode. The smaller dimension of the rectangular pinhole was aligned parallel to the plane of dispersion to produce a collimated beam with a divergence of ~1.0°. Because the diffraction line resolution is limited by the ~1.0° divergence in the scattering plane, the pinhole collimator was placed as close to the sample as possible to maximize detector resolution.

Table 1. Characteristic wavelengths

Anode	Wavelength of K_α Line (Å)	K_β Line Filter
Mo (Z = 42)	0.71	50-μm Zr
Ag (Z = 47)	0.56	25-μm Pd

X rays were detected by a thin, mirrored, P-43 X-ray-to-light converter. The optical image was transmitted to a cooled charge-coupled device camera by an 18-mm-square coherent fiber-optic bundle. A background image was subtracted from the diffraction image to generate the final, processed image.

III. PHASE TRANSITION EXPERIMENTS WITH TIN AND INDIUM

At room temperature, tin is in the β phase. The structure of the tin β phase is face-centered tetragonal with a second identical lattice offset from the original basis at coordinates (*a*,*a*,*c*)/4. The result is a diamond-like tetragonal structure with values for *c* and *a* of 3.17 Å and 5.82 Å, respectively. With this basis, X-ray reflections will occur for the same Miller indices as cubic diamond. The lowest-order reflections from a tin sample appear in Figure 2. Indium has a body-centered tetragonal structure at room temperature, with *c* = 4.95 Å and *a* = 3.25 Å. The Miller indices and scattering angles for tin and indium at X-ray wavelengths of 0.56 Å and 0.71 Å appear in Tables 2 and 3, respectively.

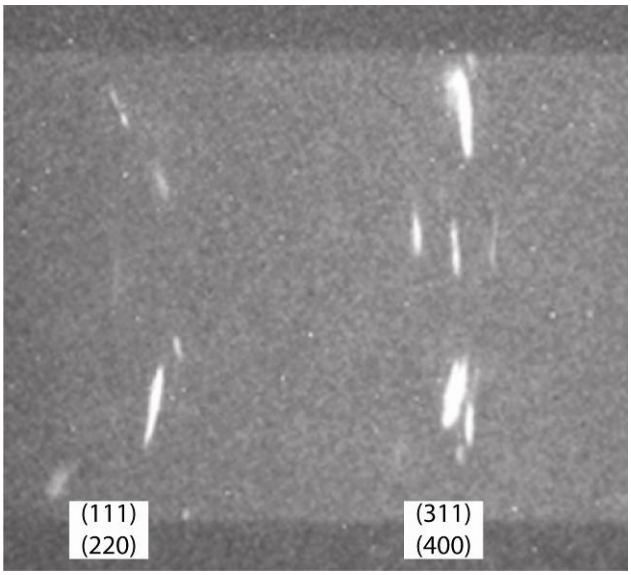

Figure 2. Lowest-order reflection from a tin sample observed with 0.71-Å pulse. A large grain size is observed.

Table 2. Tin β-phase reflections

Miller Indices	d-spacing (Å)	Scattering Angle (λ=0.71 Å)	Scattering Angle (λ=0.56 Å)
(220)	2.91	14.0°	11.1°
(111)	2.79	14.6°	11.6°
(400)	2.06	19.8°	15.7°
(311)	2.01	20.3°	16.0°

Table 3. Indium reflections

Miller Indices	d-spacing (Å)	Scattering Angle (λ=0.71 Å)	Scattering Angle (λ=0.56 Å)
(101)	2.72	15.0°	11.8°
(002)	2.48	16.5°	13.0°
(110)	2.30	17.6°	14.0°

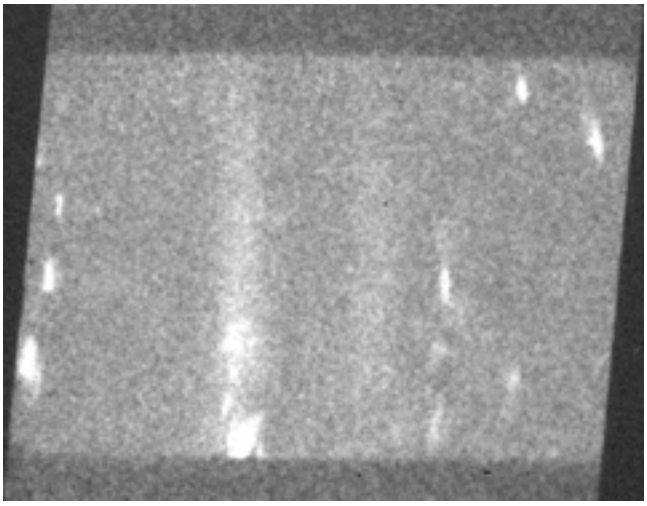

Figure 3a. Single-pulse diffraction lines at room temperature from a tin sample with a 0.56-Å silver anode. The beam is on the sample edge. The fine-grain diffraction is from the stainless-steel container.

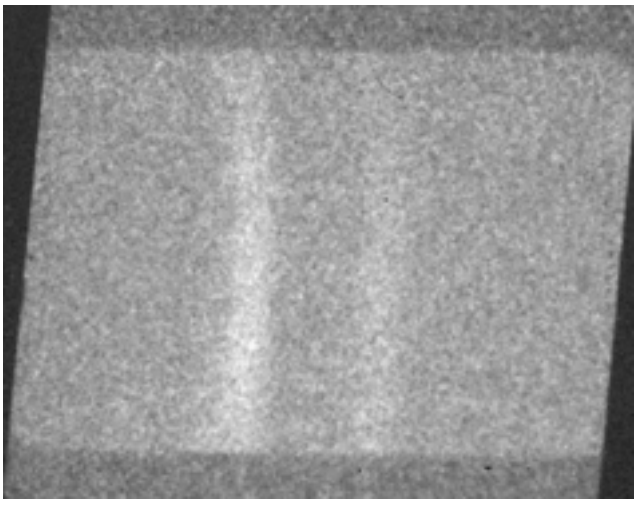

Figure 3b. Here, the temperature was raised to 230°C, above the tin melting point. The tin diffraction pattern is gone, while the stainless-steel lines are still present.

We placed samples of pressed indium and stock tin sheet on a hot plate to observe the changes in the diffraction pattern images that occur because of the solid-to-liquid phase transition. Images of the room-temperature tin samples are compared with images of liquid tin at 230°C in Figures 3a and 3b. Similar results were observed for indium.

IV. TEMPERATURE MEASUREMENTS

Coherent scattering from atomic centers in a solid-state lattice results in diffraction lines that are observed at angles for which the difference in path lengths is an integral number of wavelengths. As the temperature of a solid is raised, the displacement of the atoms in the lattice from their equilibrium position increases. This causes a random phase shift in the scattered wave front from adjacent scattering atoms. Therefore, the intensity of the diffraction lines decreases as the temperature increases, which is known as the Debye-Waller factor [2]. For a solid lattice with a single type of atom, the reduction in the diffracted X-ray intensity is given as:

$$I/I_0 = \exp-\left\{16\pi^2\langle u_s^2\rangle \sin^2\theta_B/\lambda^2\right\}, \qquad (1)$$

where $\langle u_s^2\rangle$ is the mean-square displacement of the atom position from its equilibrium position perpendicular to the Bragg plane, θ_B is the Bragg angle, and λ is the X-ray wavelength. From equation (1), we see that the reduction in intensity is greatest when the Bragg planes are closely spaced and the scattering angle is large. Using the harmonic approximation, the mean-square displacement of the atom from its equilibrium position is approximated as:

$$\langle u_S^2\rangle = \frac{3\hbar^2}{4m_a k\Theta_D}\left(\frac{\phi(x)}{x}+\frac{1}{4}\right), \qquad (2)$$

where $\hbar$ is Planck's constant, m_a is the mass of the atom, k is Boltzmann's constant, Θ_D is the Debye temperature, and $x=\Theta_D/T$, where T is the sample temperature. The term $\phi(x)$ in equation (2) is written as:

$$\phi(x) = \frac{1}{x}\int_0^x \frac{\xi\, d\xi}{\exp(\xi)-1}. \qquad (3)$$

More recent theoretical calculations consider the anharmonicity of the atomic vibrations, as well as thermal expansion [3]. However, for the initial test of our single-pulse diffraction system as a temperature diagnostic, the harmonic approximation described above should be adequate.

Because the intensity of the diffraction lines depends on the atomic mass, the Debye temperature, and the scattering angle, aluminum was chosen for the initial single-pulse diffraction tests. Aluminum has a comparatively low Debye temperature (395K) and low atomic weight (27 g/mole). Furthermore, its X-ray reflectivity is high, for wavelengths ranging from 0.56 to

0.71 Å. This allows high sensitivity to high-order reflections with large scattering angles.

For our experiments, we have used aluminum 6061-T6 0.25″ square bar stock. The sample temperature is measured using a thermistor calibrated to the melting points of indium and tin in the experiments described in section III. Shot-to-shot variations of the X-ray source intensity are approximately 10%. The results of three single-pulse (400) diffraction line observations are compared with the harmonic Debye-Waller model in Figure 4. The trend for reduced intensity with increasing temperature is apparent. The simple theoretical model shown in Figure 4 does not include anharmonic effects or the effects of thermal expansion.

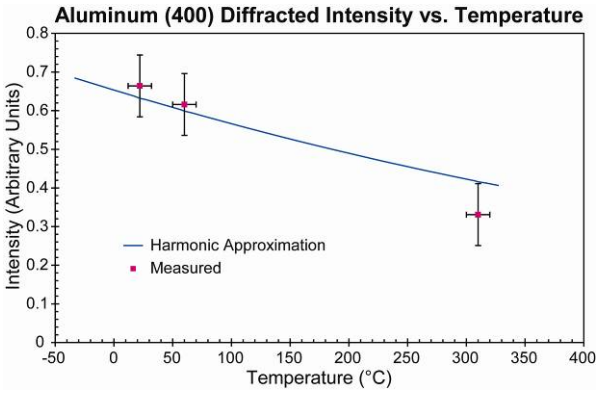

Figure 4. Measurement of the intensity variations with temperature compared with the harmonic model for 0.71-Å diffracted X-rays

V. FUTURE WORK

We expect to deploy our newly designed phase transition diagnostic on dynamic high-explosives-driven experiments in the near future. Specifically, we will attempt to observe the β-to-γ solid-solid phase transition in tin. To observe the phase transition, the sample must be shock-loaded to ~70 kbar for a time interval sufficient to perform the measurement. A vitreous carbon window will be used to provide shock-loading because it does not produce diffraction lines and because it has low attenuation for the diffraction wavelengths shown in Table 1. With a shock velocity of ~4.92 km/sec [4], shock loading will be provided for ~400 ns with a 1-mm-thick carbon window.

Furthermore, because of its proximity to the high-explosive package, the detector must be blast-protected. Work is in progress to develop blast shielding that will prevent light leaks in the detector, while allowing the X-ray wavelengths described in Table 1 to transmit through the window with minimal attenuation.

We will also develop a single-pulse, X-ray diffraction, ultrafast temperature measurements capability for dynamic experiments. This will require monitoring diffraction lines at both low and high scattering angles to correct for the shot-to-shot X-ray source variation. Bulk temperature measurements will be compared with available existing measurements.

VI. REFERENCES

[1] C. Kittel, Introduction to Solid State Physics, 6th ed. New York: John Wiley and Sons, 1986, pp. 603–605.

[2] B. E. Warren, X-ray Diffraction. New York: Dover Publications, 1990, pp. 35–38.

[3] R. M. Nicklow and R. A. Young, "Lattice Vibrations in Aluminum and the Temperature Dependence of X-ray Bragg Intensities," Phys. Rev., vol. 152, pp. 591–596.

[4] Y. M. Gupta, K. A. Zimmerman, P. A. Rigg, E. B. Zaretsky, D. M. Savage, and P. M. Bellamy, "Experimental development to obtain real-time X-ray diffraction measurements in plate impact experiments," Rev. Sci. Instrum., vol. 70, pp. 4008–4014.

Copyright Statement

This manuscript has been authored by National Security Technologies, LLC, under Contract No. DE-AC52-06NA25946 with the U.S. Department of Energy. The United States Government retains, and the publisher, by accepting the article for publication, acknowledges that the United States Government retains a nonexclusive, paid-up, irrevocable, worldwide license to publish or reproduce the published form of this manuscript, or allow others to do so, for United States Government purposes.